NASA MEMO 2-1-59L

NASA

MEMORANDUM

APPLICATION OF THE METHOD OF STEIN AND SANDERS TO THE CALCULATION OF VIBRATION CHARACTERISTICS OF A 45° DELTA-WING SPECIMEN

By John M. Hedgepeth and Paul G. Waner, Jr.

Langley Research Center
Langley Field, Va.

NATIONAL AERONAUTICS AND SPACE ADMINISTRATION
WASHINGTON
February 1959

NATIONAL AERONAUTICS AND SPACE ADMINISTRATION

MEMORANDUM 2-1-59L

APPLICATION OF THE METHOD OF STEIN AND SANDERS TO THE CALCULATION OF VIBRATION CHARACTERISTICS OF A 45° DELTA-WING SPECIMEN

By John M. Hedgepeth and Paul G. Waner, Jr.

SUMMARY

Generalized influence coefficients are calculated by the method of NACA TN 3640 for a large-scale, built-up, 45° delta-wing specimen. These are used together with appropriate generalized masses to obtain the natural modes and frequencies in symmetric and antisymmetric free-free vibration. The resulting frequencies are compared with those obtained experimentally and are found to be consistently high. Possible sources of the disparities are discussed.

INTRODUCTION

The increased importance of flutter and other aeroelastic phenomena has made the accurate determination of structural stiffness properties a necessary part of aircraft design. For this reason, the Langley Structures Research Division has been conducting a program of experimental and theoretical research of the deflection and vibration properties of built-up wing structures. One of the test structures is the large-scale 45° delta-wing specimen described in reference 1. Reference 1 also contains the details of the static and vibration tests. The experimental data obtained from this specimen have been used to assess the accuracy of two analytical methods: that of Levy (ref. 2) and the one proposed by Stein and Sanders (ref. 3). These assessments are summarized in references 4 and 5.

The purpose of the present paper is to report the details of the calculations made by the Stein-Sanders method. Influence coefficients are first computed by the procedure outlined in reference 3. These coefficients are then used in conjunction with the mass properties to find the natural modes and frequencies of free-free vibration by means of matrix iteration.

SYMBOLS

All quantities are in pound-inch-second units.

a_k	stiffness coefficient for covers (k = 0, 1, 2, 3, 4)
B_{00}, B_{01}, B_{11}	parameters defined by equation (15)
$c_1(y), c_2(y)$	trailing- and leading-edge coordinates, respectively
E	Young's modulus of elasticity
g	acceleration due to gravity
$[g]$	generalized influence-coefficient matrix
l	semispan
m	mass per unit area
m_k	generalized distributed mass (k = 0, 1, 2, 3, 4)
$\bar{m}_k$	generalized concentrated mass (k = 0, 1, 2, 3, 4)
N	tip-station index, l/ϵ
p_0, p_1, p_2	load, moment, and second moment about y-axis
w	deflection
x,y	coordinate system (fig. 1)
x_s	x-coordinate of spar
$\bar{\beta}_s$	spar or stringer stiffness parameter
γ	rib stiffness parameter
ϵ	spacing between stations
μ	parameter defined by equation (23)
Π_p	potential energy of loads

Φ_0, Φ_1, Φ_2	deflection, slope, and half-curvature at y-axis (supported structure)
Ψ_0, Ψ_1, Ψ_2	deflection, slope, and half-curvature at y-axis (free-free structure)
ω	circular frequency
$[\ ]$	rectangular matrix
$\lvert\ \rvert$	column matrix
$\lfloor\ \rfloor$	row matrix

DESCRIPTION OF SPECIMEN

A schematic drawing of the delta-wing specimen is shown in figure 1. It has a semispan of 112 inches, a root chord of 96 inches, and a leading-edge sweep of 45°. The specimen is constructed entirely of 2024 aluminum alloy which is assumed to have a Young's modulus of 10.6×10^6 psi and a Poisson's ratio of 1/3. The cover sheets are relatively thin and are stiffened by numerous stringers. There are four spanwise spars and a leading-edge spar. Closely spaced ribs provide chordwise stiffening.

The dimensions shown in figure 1 are nominal and were used in the calculations for locating stations, spars, and ribs. Precise dimensions and details of the construction and of the weight distribution of the specimen are given in reference 1. Points of interest to be noted are: the depth tapers in the spanwise direction from $5\frac{1}{2}$ inches at the carry-through section to $1\frac{3}{4}$ inches at the tip but is constant in the chordwise direction. With the exception of the leading-edge spar, all spars are unspliced for their entire length and are reinforced with heavy caps. The leading-edge spar is spliced at the center line and has no cap. The ribs are segmented, being broken at the spars. The cover sheets are of uniform thickness and are continuous across the center line. The stringers are made of equal-legged angles, are continuous across the center line, and are riveted to the outside of the covers for convenience in construction. The entire structure is symmetrical in the spanwise and depthwise directions and there are no cutouts.

CALCULATION OF GENERALIZED INFLUENCE COEFFICIENTS

In the calculations, the approach outlined in reference 3 was followed in detail. The end product is a matrix which gives the deflection φ_0, chordwise slope φ_1, and chordwise half-curvature φ_2 of the neutral surface at a number of equally spaced stations along the trailing edge (y-axis) in terms of the total load p_0, moment p_1, and second moment p_2 at each station. This generalized influence-coefficient matrix $[g]$ is obtained from the inverse of a matrix $[A]$ which is formulated from the stiffness properties of the various parts of the structure. The calculations leading to the formulation of $[A]$ are illustrated herein by following the step-by-step procedure in the section entitled "Mechanics of Application" in reference 3. The numbers in parentheses refer to the numbers of the steps in that paper, and the reader is advised to follow those steps in detail in conjunction with the present paper. All numerical values are in inch-pound units and are used with more significant figures than the actual measurements contain in order to avoid accumulated round-off errors.

(1), (2) The chosen coordinate system and stations are indicated in figure 1. The y-axis lies along the center line of the web of the rear spar and the stations are spaced at seven 16-inch intervals. Thus the stations coincide very closely with the rivet lines of every second rib. Note that the positive direction of the x-axis is opposite to that of reference 3. This change was made in order that points on the structure would have positive values of x. No change in notation is necessary except that $c_1(y)$ and $c_2(y)$ denote the x-position of the trailing edge and leading (swept) edge, respectively, instead of the reverse. Thus

$$c_1(y) = 0$$

$$c_2(y) = 96 \qquad (0 < y < 16)$$

$$c_2(y) = 112 - y \qquad (16 < y < 112)$$

(3) Because of symmetry, the neutral surface coincides with the middle surface. The stiffness properties of the spars and ribs are given in tables 2 and 3 of reference 1. The leading-edge spar (spar 5) must be treated as two separate spars 5(a) and 5(b). The area of the stringers, the z-coordinate of the centroid of the stringers, the thickness of the cover sheets, and the z-coordinate of the midplane of the cover sheets are given in table 1 of reference 1. The x-coordinates of the stringers can be found from figure 2 of reference 1 if 5.25 inches is used as the

distance between the center line of the rear spar and the rivet line of the rearmost stringer.

(4) The required values of the cover stiffness parameters $a_{k,n}$ and $a_{k,n+\frac{1}{2}}$ are given in table I. They and all succeeding values of stiffness have been divided by E, which factor will ultimately reappear as a multiplier on the generalized influence-coefficient matrix.

(5), (6), (7) The values of effective stiffness $\bar{\beta}_{s,n}$ and location $x_{s,n}$ for the swept spar 5(b) are given in table II. The contributions of the unswept spars and the stringers are included in the combined fashion suggested in step (10) of reference 3. Consequently, the summed quantities $\sum \bar{\beta}_{s,n}$, $\sum \bar{\beta}_{s,n}x_{s,n}$, $\sum \bar{\beta}_{s,n}x_{s,n}^2$, $\sum \bar{\beta}_{s,n}x_{s,n}^3$ and $\sum \bar{\beta}_{s,n}x_{s,n}^4$ are listed in table II.

(8) The values of the rib stiffness parameter γ for each rib are given in table III; the ribs are numbered in accordance with their station locations, either on or halfway between stations. It should be noted that the rib stiffnesses have been reduced somewhat (about 5 percent) below those in reference 1 in order to account for the ribs' being broken at the spars.

From the foregoing quantities, the matrix $[A]$ can be set up, inverted, and modified to obtain the $[g]$ matrix. Tables IV(a) and IV(b) show the results for the cases of symmetric deformation and antisymmetric deformation, respectively. In either case,

$$|\varphi| = [g]|p| \tag{1}$$

For symmetric deformation $|\varphi|$ is a 24-element column matrix: eight φ_0's, eight φ_1's, and eight φ_2's for stations 0 through 7. The column matrix $|p|$ is similarly made up of eight p_0's, p_1's, and p_2's. For antisymmetric deformation $|\varphi|$ and $|p|$ are 21-element matrices, the quantities at the center line not appearing because they are always zero. Note that the boundary conditions specified in reference 3 require that $\varphi_{0,0}$ and $\varphi_{1,0}$ be zero in the symmetric case and that $\varphi_{0,1}$ be zero in the antisymmetric case. Space has been provided for these quantities in the matrix formulation in order to allow the introduction of rigid-body

motions necessary for the analysis of free-free vibrations. At this point, the rows of zeros in the $[g]$ matrices are sufficient to satisfy the boundary conditions on the supported structure.

DETERMINATION OF GENERALIZED MASS MATRIX

In this section, the calculation of the generalized mass matrix needed for the determination of vibration modes and frequencies is outlined. Since the mechanics of the application of the Stein-Sanders approach to vibration problems has not heretofore been described, a detailed treatment is desirable here.

As has been pointed out in reference 3, the generalized loads $p_{k,n}$ are given in terms of the potential energy of the applied loads Π_p by

$$p_{k,n} = - \frac{\partial \Pi_p}{\partial \psi_{k,n}} \tag{2}$$

where, for sinusoidal natural vibration,

$$\Pi_p = - \frac{\omega^2}{2g} \int_0^l \int_{c_1}^{c_2} mw^2 dx\, dy = - \frac{\omega^2}{2g} \int_0^l \int_{c_1}^{c_2} m\left(\psi_0 + x\psi_1 + x^2\psi_2\right)^2 dx\, dy \tag{3}$$

Note that $w = \psi_0 + x\psi_1 + x^2\psi_2$, where the ψ_k's are the actual generalized deflections which include possible rigid-body motions. The use of $\psi_{k,n}$ in equation (2), rather than $\varphi_{k,n}$ as was employed in reference 3, is valid here since the relation between the inertia loading and the vibration amplitude is independent of the particular boundary conditions on the structure. Carrying out the integration in the chordwise direction yields

$$\Pi_p = - \frac{\omega^2}{2g} \int_0^l \left[m_0 \psi_0^2 + m_1\left(2\psi_0\psi_1\right) + m_2\left(2\psi_0\psi_2 + \psi_1^2\right) + 2m_3\psi_1\psi_2 + m_4\psi_2^2 \right] dy \tag{4}$$

where

$$m_k = \int_{c_1}^{c_2} mx^k dx \tag{5}$$

The functions m_k are not, in general, continuous. Such things as structural discontinuities and fuel cells will produce finite discontinuities in m_k; concentrated masses and ribs will produce impulse-type discontinuities. It is convenient to assume temporarily that there are no discontinuities, and then to correct for their effects subsequently. Thus, for continuous m_k, trapezoidal integration of equation (4) gives

$$\Pi_p = -\frac{\omega^2\epsilon}{2g}\left(\frac{1}{2}m_{0,0}\psi_{0,0}^2 + m_{0,1}\psi_{0,1}^2 + \cdots + m_{0,N-1}\psi_{0,N-1} + \frac{1}{2}m_{0,N}\psi_{0,N}^2 + \right.$$
$$m_{1,0}\psi_{0,0}\psi_{1,0} + 2m_{1,1}\psi_{0,1}\psi_{1,1} + \cdots + 2m_{1,N-1}\psi_{0,N-1}\psi_{1,N-1} + m_{1,N}\psi_{0,N}\psi_{1,N} +$$
$$\cdots\cdots\cdots\cdots\cdots\cdots\cdots\cdots\cdots\cdots\cdots\cdots\cdots\cdots +$$
$$\left.\frac{1}{2}m_{4,0}\psi_{2,0}^2 + m_{4,1}\psi_{2,1}^2 + \cdots + m_{4,N-1}\psi_{2,N-1}^2 + \frac{1}{2}m_{4,N}\psi_{2,N}^2\right) \tag{6}$$

where the equally spaced stations are numbered from 0 at the center line to N at the tip.

Using equation (2) yields

$$\left|p_0\right| = \frac{\omega^2}{g}\left\{\begin{bmatrix}\frac{\epsilon}{2}m_{0,0} & \epsilon m_{0,1} & \cdots & \epsilon m_{0,N-1} & \frac{\epsilon}{2}m_{0,N}\end{bmatrix}\left|\psi_0\right| + \right.$$
$$\begin{bmatrix}\frac{\epsilon}{2}m_{1,0} & \epsilon m_{1,1} & \cdots & \epsilon m_{1,N-1} & \frac{\epsilon}{2}m_{1,N}\end{bmatrix}\left|\psi_1\right| +$$
$$\left.\begin{bmatrix}\frac{\epsilon}{2}m_{2,0} & \epsilon m_{2,1} & \cdots & \epsilon m_{2,N-1} & \frac{\epsilon}{2}m_{2,N}\end{bmatrix}\left|\psi_2\right|\right\} \tag{7}$$

and p_1 and p_2 can be expressed in a similar fashion.

Thus,

$$\begin{vmatrix} p_0 \\ p_1 \\ p_2 \end{vmatrix} = \frac{\omega^2}{g} \begin{bmatrix} M_0 & M_1 & M_2 \\ M_1 & M_2 & M_3 \\ M_2 & M_3 & M_4 \end{bmatrix} \begin{vmatrix} \psi_0 \\ \psi_1 \\ \psi_2 \end{vmatrix} \tag{8}$$

or

$$\left| p \right| = \frac{\omega^2}{g} \left[M \right] \left| \psi \right| \tag{9}$$

where the M_k are $(N + 1) \times (N + 1)$ matrices. The contribution of the continuous m_k to these matrices is given by

$$\begin{bmatrix} \frac{\epsilon}{2} m_{k,0} & & & & \\ & \epsilon m_{k,1} & & & \\ & & \cdots & & \\ & & & \epsilon m_{k,N-1} & \\ & & & & \frac{\epsilon}{2} m_{k,N} \end{bmatrix}$$

A finite discontinuity in m_k can be handled in several ways, but the simplest is merely to alter the value of m_k at the station nearest the discontinuity. This can be done in precisely the same manner as is outlined for discontinuous a_k in step (4) of the step-by-step procedure in reference 3.

The energy due to a concentrated mass or a rib mass located at a distance ϵd to the right of station j is

$$\begin{aligned} \Pi_p = -\frac{\omega^2}{2g} \Big\{ & \bar{m}_0 \left[(1 - d)\psi_{0,j} + d\psi_{0,j+1} \right]^2 + 2\bar{m}_1 \left[(1 - d)\psi_{0,j} + d\psi_{0,j+1} \right] \left[(1 - d)\psi_{1,j} + d\psi_{1,j+1} \right] + \\ & 2\bar{m}_2 \left[(1 - d)\psi_{0,j} + d\psi_{0,j+1} \right] \left[(1 - d)\psi_{2,j} + d\psi_{2,j+1} \right] + \bar{m}_2 \left[(1 - d)\psi_{1,j} + d\psi_{1,j+1} \right]^2 + \\ & 2\bar{m}_3 \left[(1 - d)\psi_{1,j} + d\psi_{1,j+1} \right] \left[(1 - d)\psi_{2,j} + d\psi_{2,j+1} \right] + \bar{m}_4 \left[(1 - d)\psi_{2,j} + d\psi_{2,j+1} \right]^2 \Big\} \end{aligned}$$

where the $\bar{m}_k$'s are integrals across the chord analogous to those defining m_k. Note that linear interpolation has been used to specify the values of ψ_n between stations. Using equation (2) gives

$$\left.\begin{aligned} p_{0,j} &= \frac{\omega^2}{g}\Big\{(1-d)^2\bar{m}_0\psi_{0,j} + d(1-d)\bar{m}_0\psi_{0,j+1} + (1-d)^2\bar{m}_1\psi_{1,j} + d(1-d)\bar{m}_1\psi_{1,j+1} + \\ &\qquad (1-d)^2\bar{m}_2\psi_{2,j} + d(1-d)\bar{m}_2\psi_{2,j+1}\Big\} \\ p_{0,j+1} &= \frac{\omega^2}{g}\Big\{d(1-d)\bar{m}_0\psi_{0,j} + d^2\bar{m}_0\psi_{0,j+1} + d(1-d)\bar{m}_1\psi_{1,j} + d^2\bar{m}_1\psi_{1,j+1} + \\ &\qquad d(1-d)\bar{m}_2\psi_{2,j} + d^2\bar{m}_2\psi_{2,j+1}\Big\} \end{aligned}\right\} \quad (10)$$

and so forth. Thus it can be seen that the effects of the concentration can be incorporated by including in each $[\bar{M}_k]$ matrix a block of terms like

$$\begin{matrix} (1-d)^2\bar{m}_k & d(1-d)\bar{m}_k \\ d(1-d)\bar{m}_k & d^2\bar{m}_k \end{matrix}$$

The upper left-hand element is to be located in the $(j+1)$ row and column. All the concentrations are handled in this manner.

For the delta-wing specimen under consideration the generalized mass matrix is given in table V. The computed numbers are based on the mass (weight) data given in tables 2, 4, and 5 and figure 4 of reference 1. The generalized mass matrix also includes the masses of shaker armatures (2.0 pounds each) and pickups (0.7 pound each) located as shown in figure 10 of reference 1.

In order to determine free-free modes and frequencies, the constraining conditions used in obtaining the influence coefficients must be relaxed. The freeing procedure leading to the calculation of these vibration characteristics is discussed in the next section.

FREE-FREE VIBRATION ANALYSIS

Symmetric Modes

For symmetric free-free vibration the actual generalized deflection ψ_n is related to the constrained generalized deflection φ_n by the following matrix equation:

$$|\psi| = |\varphi| + \psi_{0,0}|I_0| + \psi_{1,0}|I_1| \tag{11}$$

where $|I_0|$ and $|I_1|$ are (for the present structure) 24-element columns. The first eight elements of $|I_0|$ are equal to 1 and all others are 0; the second eight elements of $|I_1|$ are 1 and the rest are 0. The term $\psi_{0,0}|I_0|$ thus allows rigid-body translation; the term $\psi_{1,0}|I_1|$ allows rigid-body pitching.

Expressing $|\varphi|$ in terms of $|p|$ (eq. (1)) and then $|p|$ in terms of $|\psi|$ (eq. (9)) yields

$$|\psi| = \frac{\omega^2}{g}[g][M]|\psi| + \psi_{0,0}|I_0| + \psi_{1,0}|I_1| \tag{12}$$

The unknowns $\psi_{0,0}$ and $\psi_{1,0}$ can be found from the conditions for self-equilibration of the inertia loading; that is,

$$\left.\begin{aligned} \lfloor I_0 \rfloor |p| &= 0 \\ \lfloor I_1 \rfloor |p| &= 0 \end{aligned}\right\} \tag{13}$$

where the rows $\lfloor I_0 \rfloor$ and $\lfloor I_1 \rfloor$ are the transposes of the corresponding columns. Multiplying equation (12) by $[M]$ and then by $\lfloor I_0 \rfloor$ and $\lfloor I_1 \rfloor$ gives, respectively,

$$\left.\begin{aligned} 0 &= \frac{\omega^2}{g}\lfloor I_0 \rfloor [M][g][M]|\psi| + B_{00}\psi_{0,0} + B_{01}\psi_{1,0} \\ 0 &= \frac{\omega^2}{g}\lfloor I_1 \rfloor [M][g][M]|\psi| + B_{10}\psi_{0,0} + B_{11}\psi_{1,0} \end{aligned}\right\} \tag{14}$$

where the left-hand sides are 0 by virtue of equation (13) and

$$\left.\begin{aligned} B_{00} &= \lfloor I_0 \rfloor [M] |I_0| \\ B_{01} &= B_{10} \\ &= \lfloor I_0 \rfloor [M] |I_1| \\ B_{11} &= \lfloor I_1 \rfloor [M] |I_1| \end{aligned}\right\} \tag{15}$$

Note that B_{00} is half the mass of the specimen, B_{01} is half the mass moment of the specimen about the trailing edge, and B_{11} is half the mass moment of inertia of the specimen about the trailing edge.

Equations (14) can be solved for $\psi_{0,0}$ and $\psi_{1,0}$. The result is

$$\left.\begin{aligned} \psi_{0,0} &= \frac{\omega^2}{g\left(B_{00}B_{11} - B_{01}^2\right)}\left(B_{01}\left[I_1\right] - B_{11}\left[I_0\right]\right)[M][g][M]|\psi| \\ \psi_{1,0} &= \frac{\omega^2}{g\left(B_{00}B_{11} - B_{01}^2\right)}\left(B_{01}\left[I_0\right] - B_{00}\left[I_1\right]\right)[M][g][M]|\psi| \end{aligned}\right\} \tag{16}$$

Substitution of $\psi_{0,0}$ and $\psi_{1,0}$ into equation (12) yields, finally,

$$|\psi| = \frac{\omega^2}{g}\left\{[I] + [F_S]\right\}[g][M]|\psi| \tag{17}$$

where $[I]$ is the identity matrix and

$$[F_S] = \frac{1}{B_{00}B_{11} - B_{01}^2}\left\{B_{01}|I_0|\left[I_1\right] + B_{01}|I_1|\left[I_0\right] - B_{00}|I_1|\left[I_1\right] - B_{11}|I_0|\left[I_0\right]\right\}[M] \tag{18}$$

Equation (17) is in a suitable form to be handled by standard iteration techniques in order to calculate the natural modes and frequencies.

Antisymmetric Modes

For antisymmetrical free-free vibration, the following relationship exists:

$$|\psi| = |\varphi| + \psi_{0,1}|r| \tag{19}$$

where $|r|$ is (for the present structure) a 21-element column with the first seven elements equal to the integers from 1 to 7 and the other elements equal to 0. The term $\psi_{0,1}|r|$ allows freedom of rigid-body rolling.

Using equations (1) and (9) gives

$$|\psi| = \frac{\omega^2}{g}[g][M]|\psi| + \psi_{0,1}|r| \tag{20}$$

Note that in this case $[M]$ is a matrix of twenty-first order obtained from the one in table V by deleting the first, ninth, and seventeenth rows and columns of that matrix. It should be recalled that this reduction of order comes about because the generalized deflections at the center line (station zero) are necessarily zero.

Self-equilibrium of the inertia rolling moments requires that

$$\lfloor r \rfloor |p| = 0 \tag{21}$$

or

$$0 = \frac{\omega^2}{g} \lfloor r \rfloor [M][g][M]|\psi| + \mu\psi_{0,1} \tag{22}$$

where

$$\mu = \lfloor r \rfloor [M]|r| \tag{23}$$

is the mass moment of the half-span about the center line.

Solving for $\psi_{0,1}$ and substituting in equation (20) gives

$$|\psi| = \frac{\omega^2}{g} \left\{ [I] + [F_A] \right\} [g][M]|\psi| \tag{24}$$

where

$$[F_A] = - \frac{|r| \lfloor r \rfloor [M]}{\mu} \tag{25}$$

Equation (24) is in a form suitable for iteration.

RESULTS AND DISCUSSION

The first four modes and frequencies for free-free symmetric and antisymmetric vibration were calculated by matrix iteration from equations (17) and (24). The results are given in tables VI and VII and in figure 2. In table VI are shown the frequencies obtained from the Stein-Sanders method, the frequencies measured experimentally (ref. 1), and the percentage difference. In table VII are shown the calculated mode shapes. These are given in terms of the values of ψ_k at each station for each mode. The node-line patterns for the various modes are shown in figure 2. The node-line locations at each station were calculated from the equation

$$\psi_0 + x\psi_1 + x^2\psi_2 = 0$$

Also shown for comparison are the node-line patterns obtained experimentally (ref. 1).

As shown by figure 2, the node lines calculated by the Stein-Sanders method agree extremely well with those obtained experimentally. On the other hand, the errors in the calculated frequencies shown in table VI are large, especially for the higher modes. These errors are most probably due to inaccuracies in the generalized influence coefficients; these inaccuracies, in turn, arise from basic shortcomings of the Stein-Sanders method when applied to this particular structure. The most serious of these are the lack of enough freedom in the chordwise shape of the deflection and the neglect of the effects of transverse shear. The magnitude of these effects can be visualized from the comparison of theoretical and experimental static deflections under a uniform load shown in figure 3.

Figure 3(a) shows the deflections along the odd-numbered stations due to a uniform loading of 1 psi for the specimen mounted on the three-point support used in the experiment (ref. 1). Figure 3(b) shows the deflections for the specimen cantilevered at the root chord. The theoretical deflections were calculated from generalized influence coefficients modified for the different support conditions by the procedure outlined in appendix A of reference 3. The experimental deflections were calculated from the experimental influence coefficients tabulated in reference 1.

Figure 3 shows large errors in the theoretical deflections, particularly in the region close to the center line. Here the curvatures in the chordwise direction are large. Going from the three-point support to the cantilever support greatly reduces the magnitude of the curvature in the chordwise direction and improves the theoretical results, as can be seen from the solid curves in figure 4. Further improvement results from including approximately the effects of transverse shear, as illustrated by the long-and-short-dashed curves. The transverse-shear corrections, which were obtained merely by adding the shear deflections of the structure treated as a beam to the solid-line deflections, bring the theoretical results into excellent agreement with the experimental results.

CONCLUDING REMARKS

The poor agreement between theoretical and experimental vibration frequencies indicates that the Stein-Sanders method is unsatisfactory for the analysis of the particular delta-wing specimen treated herein. To conclude that the method is unsatisfactory for more realistic structures, however, would be erroneous since the present specimen had no

extra stiffening in the chordwise direction such as would be afforded by the fuselage in an actual case. The static-deflection results imply that a significant improvement in the accuracy would result from such stiffening. On the other hand, substantial errors due to tranverse-shear effects would still occur unless these effects were incorporated into the analysis.

Langley Research Center,
National Aeronautics and Space Administration,
Langley Field, Va., October 22, 1958.

REFERENCES

1. Kordes, Eldon E., Kruszewski, Edwin T., and Weidman, Deene J.: Experimental Influence Coefficients and Vibration Modes of a Built-Up 45° Delta-Wing Specimen. NACA TN 3999, 1957.

2. Levy, Samuel: Structural Analysis and Influence Coefficients for Delta Wings. Jour. Aero. Sci., vol. 20, no. 7, July 1953, pp. 449-454.

3. Stein, Manuel, and Sanders, J. Lyell, Jr.: A Method for Deflection Analysis of Thin Low-Aspect-Ratio Wings. NACA TN 3640, 1956.

4. Hedgepeth, John M.: Recent Research on the Determination of Natural Modes and Frequencies of Aircraft Wing Structures. Rep. 37, AGARD, North Atlantic Treaty Organization (Paris), Apr. 1956.

5. Kruszewski, Edwin T., Kordes, Eldon E., and Weidman, Deene J.: Theoretical and Experimental Investigations of Delta-Wing Vibrations. NACA TN 4015, 1957.

TABLE I

COVER STIFFNESS PARAMETERS

Station, n	$\frac{a_{0,n}}{E}$	$\frac{a_{1,n}}{E}$	$\frac{a_{2,n}}{E}$	$\frac{a_{3,n}}{E}$	$\frac{a_{4,n}}{E}$	$\frac{a_{0,n+\frac{1}{2}}}{E}$	$\frac{a_{1,n+\frac{1}{2}}}{E}$	$\frac{a_{2,n+\frac{1}{2}}}{E}$
0	110.833	5,319.95	340,477	24,514,400	1,882,700,000	110.833	5,319.95	340,477
1	110.833	5,319.95	340,477	24,514,400	1,882,700,000	90.2631	3,971.57	232,999
2	72.3635	2,894.54	154,375	9,262,530	592,802,000	56.9509	2,050.23	98,411.1
3	43.8425	1,402.96	59,859.7	2,873,270	147,111,000	32.8557	919.960	34,345.2
4	23.8077	571.384	18,284.3	658,234	25,276,200	16.5156	330.313	8,808.34
5	10.7969	172.750	3,685.34	88,448.2	2,264,280	6.46871	77.6245	1,241.99
6	3.34832	26.7866	285.724	3,428.68	43,887.2	1.25300	5.01200	26.7307
7	0	0	0	0	0	---	---	---

TABLE II

SPAR STIFFNESS PARAMETERS

Station, n	Spar 5(b)		Unswept spars and stringers				
	$\bar{\beta}_{s,n}$	$x_{s,n}$	$\sum \bar{\beta}_{s,n}$	$\sum \bar{\beta}_{s,n} x_{s,n}$	$\sum \bar{\beta}_{s,n} x_{s,n}^2$	$\sum \bar{\beta}_{s,n} x_{s,n}^3$	$\sum \bar{\beta}_{s,n} x_{s,n}^4$
0	0	112	76.318	3,266.77	200,171	14,026,000	1,041,200,000
1	.406691	96	76.318	3,266.77	200,171	14,026,000	1,041,200,000
2	.607404	80	51.8745	1,869.85	96,089.0	5,543,270	342,287,000
3	.437386	64	33.6900	1,014.84	43,691.3	2,090,960	106,231,000
4	.300299	48	18.5807	416.200	13,909.4	522,016	20,954,800
5	.193115	32	8.59570	117.235	2,489.05	58,518.8	1,457,650
6	.112809	16	2.63250	19.8607	221.142	2,692.38	34,649.9
7	.056350	0	.269720	0	0	0	0

TABLE III

RIB STIFFNESS PARAMETERS

Station, n	$\frac{\gamma_n}{E}$	$\frac{\gamma_{n+\frac{1}{2}}}{E}$
0	193.170	386.339
1	1115.42	299.974
2	228.971	174.647
3	127.304	89.9428
4	63.1952	40.9168
5	24.7148	14.5403
6	7.10490	2.34160
7	0	---------

TABLE IV.- GENERALIZED INFLUENCE-COEFFICIENT MATRIX

(a) Symmetrical Deformation

$$\left[g\right] = \frac{\epsilon^3}{E}\begin{bmatrix} g_{00} & g_{01} & g_{02} \\ g_{10} & g_{11} & g_{12} \\ g_{20} & g_{21} & g_{22} \end{bmatrix}; \quad g_{ij} = g_{ji}$$

$g_{00} = 10^{-2}$

0	0	0	0	0	0	0	0
0	1.4605	2.3371	2.9633	3.4715	3.9320	4.3812	4.8134
0	2.3371	6.2959	9.0016	11.1183	12.9979	14.8160	16.5740
0	2.9633	9.0016	16.5142	22.0266	26.7453	31.2486	35.6145
0	3.4715	11.1183	22.0266	34.8672	44.9403	54.2410	63.2448
0	3.9320	12.9979	26.7453	44.9403	66.4296	84.4999	101.7525
0	4.3812	14.8160	31.2486	54.2410	84.4999	121.7644	154.7403
0	4.8134	16.5740	35.6145	63.2448	101.7525	154.7403	230.3527

$g_{01} = 10^{-4}$

0	0	0	0	0	0	0	0
0	-5.2356	-7.3041	-8.1018	-8.3574	-8.4477	-8.6696	-8.6415
0	-7.3528	-18.4467	-22.7682	-24.1506	-24.5853	-25.3639	-25.2526
0	-8.2481	-23.0549	-40.2180	-45.6460	-47.0877	-48.7870	-48.4920
0	-8.6298	-24.8620	-46.4386	-71.4180	-77.3319	-80.6397	-79.8611
0	-8.8514	-25.7484	-48.8833	-79.1175	-116.6625	-125.3510	-122.8877
0	-9.0593	-26.4959	-50.6333	-82.8500	-126.8145	-191.9687	-182.5040
0	-9.2374	-27.1494	-52.1841	-86.0003	-133.1657	-205.4808	-286.4404

$g_{02} = 10^{-6}$

0	0	0	0	0	0	0	0
-4.5894	-0.3323	0.9345	0.9774	0.5543	0.1588	0.6541	0.0363
-10.4855	-4.8743	3.0949	4.2470	2.5854	0.7063	2.0006	-0.4154
-16.4006	-10.5071	-0.7644	10.1746	7.8673	2.5061	3.8709	-2.3061
-21.7915	-16.0319	-6.5318	5.2467	19.6448	9.0176	6.3516	-9.0831
-26.5575	-21.0319	-12.3566	-2.4834	9.9552	30.4915	10.8050	-37.3008
-30.9116	-25.6066	-17.7943	-10.1823	-3.3790	5.2410	48.4020	-176.2185
-35.0030	-29.9262	-22.9798	-17.5840	-16.4639	-23.7835	-44.7327	-733.9283

$g_{11} = 10^{-6}$

0	0	0	0	0	0	0	0
0	28.3524	37.9775	40.3652	39.9856	39.1644	39.1042	39.0262
0	37.9775	95.1750	111.8504	112.2741	109.1631	108.4191	108.0850
0	40.3652	111.8504	204.3501	218.2796	210.5924	206.4018	205.3515
0	39.9856	112.2741	218.2796	372.4092	372.8470	356.8939	353.0658
0	39.1644	109.1631	210.5924	372.8470	667.7383	634.3781	616.0558
0	39.1042	108.4191	206.4018	356.8939	634.3781	1,327.3634	1,236.7512
0	39.0262	108.0850	205.3515	353.0658	616.0558	1,236.7512	7,756.8221

$g_{12} = 10^{-8}$

0	0	0	0	0	0	0	0
25.8394	-1.4518	-9.8037	-9.9815	-6.7716	-3.3508	-2.7615	-2.0778
53.9159	18.0223	-35.8236	-43.4052	-30.6770	-14.8455	-9.1998	-6.4535
78.6843	41.3218	-24.2851	-115.1064	-98.2423	-51.0132	-23.9552	-16.8594
97.5257	61.3070	-2.7311	-102.7624	-275.8926	-179.4049	-68.4267	-40.1844
109.6814	74.8382	14.8797	-74.3519	-242.4892	-666.7485	-253.1988	-50.2044
117.1688	82.8651	25.0295	-55.9268	-193.0163	-525.2459	-1,954.3729	37.4970
116.9185	82.6621	24.9975	-55.3751	-189.3031	-498.6749	-1,808.3827	49,693.9410

$g_{22} = 10^{-10}$

159.4650	131.6396	100.0772	69.7104	43.9338	24.5883	6.5715	21.2506
131.6396	132.8083	110.6374	80.9280	51.9840	28.9754	9.3431	24.4307
100.0772	110.6374	138.8273	118.6105	80.3315	44.0332	16.3945	32.7155
69.7104	80.9280	118.6105	210.1371	171.7124	97.7948	37.5284	58.8470
43.9338	51.9840	80.3315	171.7124	459.4673	324.9323	122.8315	148.5812
24.5883	28.9754	44.0332	97.7948	324.9323	1417.3669	597.8610	461.6689
6.5715	9.3431	16.3945	37.5284	122.8315	597.8610	6,995.8497	3,673.1493
21.2506	24.4307	32.7155	58.8470	148.5812	461.6689	3,673.1493	511,957.79

TABLE IV.- GENERALIZED INFLUENCE-COEFFICIENT MATRIX - Concluded

(b) Antisymmetrical Deformation

$$[g] = \frac{\epsilon^3}{E}\begin{vmatrix} g_{00} & g_{01} & g_{02} \\ g_{10} & g_{11} & g_{12} \\ g_{20} & g_{21} & g_{22} \end{vmatrix}; \quad g_{ij} = g_{ji}$$

$g_{00} = 10^{-2}$

0	0	0	0	0	0	0
0	2.57123	4.36403	5.83200	7.20010	8.55431	9.91682
0	4.36403	10.9163	15.9004	20.3374	24.6510	28.9694
0	5.83200	15.9004	28.5161	38.7284	48.3060	57.8162
0	7.20010	20.3374	38.7284	60.8982	79.8337	98.2626
0	8.55431	24.6510	48.3060	79.8337	118.5971	153.4663
0	9.91682	28.9694	57.8162	98.2626	153.4663	231.7661

$g_{01} = 10^{-4}$

0	0	0	0	0	0	0
1.79887	-4.53310	-6.08128	-5.78413	-5.15891	-4.74374	-4.72819
4.61612	-2.40976	-14.3545	-16.2288	-15.2881	-14.4178	-14.3140
8.03087	2.74318	-11.0121	-30.4154	-32.4931	-31.6401	-31.1675
11.7777	9.04169	-3.65303	-26.2776	-58.5211	-61.5330	-59.4878
15.6755	15.6450	4.56756	-17.9999	-55.1910	-113.1384	-104.2097
19.6327	22.3059	12.8404	-9.42059	-48.4080	-112.0715	-193.6732

$g_{02} = 10^{-6}$

0	0	0	0	0	0	0
0.0490400	5.96449	6.36279	4.39499	2.11223	0.506115	0.880214
0.115012	7.32222	16.6890	13.0266	6.0558	1.03498	0.696020
0.186129	6.90149	16.3851	28.3729	14.8358	1.72992	-4.31509
0.257123	6.06107	13.0697	22.1589	38.5729	4.83003	-30.3993
0.326777	5.26017	9.53703	12.1339	15.4922	41.0693	-167.0757
0.395885	4.53113	6.22020	2.38588	-11.3255	-53.2766	-722.6711

$g_{11} = 10^{-6}$

12.7550	20.4739	25.7624	29.5069	32.0013	33.6062	33.4978
20.4739	73.8791	91.9924	95.6147	95.2772	95.2198	94.9139
25.7624	91.9924	183.3723	198.1404	191.5197	186.0352	185.1218
29.5069	95.6147	198.1404	350.7493	350.4543	330.9064	327.3572
32.0013	95.2772	191.5197	350.4543	643.2705	605.0374	587.0817
33.6062	95.2198	186.0352	330.9064	605.0374	1,291.820	1,201.730
33.4978	94.9139	185.1218	327.3572	587.0817	1,201.730	7,722.306

$g_{12} = 10^{-8}$

0.357139	2.51667	4.23019	4.88730	4.53501	2.48129	6.66447
0.416251	-35.7211	-35.9270	-22.0109	-7.57499	-0.649586	3.97644
0.372644	-42.3980	-119.9726	-96.6797	-46.7637	-11.9076	-6.58982
0.304273	-37.4011	-119.2887	-281.2345	-178.1168	-52.0014	-30.0105
0.250619	-31.1834	-98.9304	-252.5471	-667.5713	-235.6573	-41.7332
0.222539	-27.4213	-84.4719	-204.4838	-526.4627	-1,935.246	43.6259
0.222330	-27.3427	-83.9134	-200.8741	-500.0124	-1,789.626	-49,687.76

$g_{22} = 10^{-10}$

-0.376591	-0.437242	-0.364781	-0.245316	-0.136065	-0.0606687	-0.103730
-0.437242	43.2112	47.7417	34.7671	18.8111	6.86534	11.6145
-0.364781	47.7417	157.5055	138.0318	79.2549	28.5229	43.0942
-0.245316	34.7671	138.0318	438.0681	313.1202	113.7636	137.7855
-0.136065	18.8111	79.2549	313.1202	1,411.054	593.1698	457.5185
-0.0606687	6.86534	28.5229	113.7636	593.1698	6,992.212	3,676.822
-0.103730	11.6145	43.0942	137.7855	457.5185	3,676.822	511,958.0

TABLE V.- GENERALIZED MASS MATRIX

$$[M] = \begin{bmatrix} M_0 & M_1 & M_2 \\ M_1 & M_2 & M_3 \\ M_2 & M_3 & M_4 \end{bmatrix}$$

$$[M_0] = 10^2 \begin{bmatrix} 0.235241 & 0.00866976 & 0.00749406 & 0.0156380 & 0.00371561 & 0.00230240 & 0.00794062 & 0.00029090 \\ 0.00866976 & 0.566361 & 0.405841 & 0.331152 & 0.262650 & 0.171364 & 0.0850829 & 0.0164161 \\ 0.00749406 & 0.00866976 & 0.0156380 & 0.00371561 & 0.00230240 & 0.00794062 & 0.00029090 & \end{bmatrix}$$

$$[M_1] = 10^4 \begin{bmatrix} 0.109628 & 0.00413195 & 0.00326729 & 0.00600933 & 0.00103621 & 0.000456808 & 0.000562874 & 0.000011352 \\ 0.00413195 & 0.263605 & 0.159436 & 0.106107 & 0.0631075 & 0.0261948 & 0.00679925 & 0.000011352 \\ 0.00326729 & 0.00413195 & 0.00600933 & 0.00103621 & 0.000456808 & 0.000562874 & 0.000011352 & \end{bmatrix}$$

$$[M_2] = 10^6 \begin{bmatrix} 0.0708200 & 0.00264212 & 0.00191089 & 0.00308688 & 0.000387517 & 0.000121669 & 0.000123796 & 0.0000006055 \\ 0.00264212 & 0.170392 & 0.0866876 & 0.0472525 & 0.0218966 & 0.00599939 & 0.000868914 & 0.0000006055 \\ 0.00191089 & 0.00264212 & 0.00308688 & 0.000387517 & 0.000121669 & 0.000123796 & 0.0000006055 & \end{bmatrix}$$

$$[M_3] = 10^8 \begin{bmatrix} 0.0516767 & 0.00190236 & 0.00125791 & 0.00173128 & 0.000162877 & 0.0000364213 & 0.0000283558 & 0.0000000363264 \\ 0.00190236 & 0.124340 & 0.0529313 & 0.0235032 & 0.00850026 & 0.00151570 & 0.000126736 & 0.0000000363264 \\ 0.00125791 & 0.00190236 & 0.00173128 & 0.000162877 & 0.0000364213 & 0.0000283558 & 0.0000000363264 & \end{bmatrix}$$

$$[M_4] = 10^{10} \begin{bmatrix} 0.0403924 & 0.00146221 & 0.000883788 & 0.00103044 & 0.0000729919 & 0.0000116294 & 0.00000661025 & 0.000000002325 \\ 0.00146221 & 0.0971812 & 0.0345499 & 0.0124523 & 0.00351850 & 0.000405174 & 0.0000203251 & 0.000000002325 \\ 0.000883788 & 0.00146221 & 0.00103044 & 0.0000729919 & 0.0000116294 & 0.00000661025 & 0.000000002325 & \end{bmatrix}$$

TABLE VI.- COMPARISON OF VIBRATION FREQUENCIES

Mode	Symmetric modes			Antisymmetric modes		
	Frequency, cps		Error, percent	Frequency, cps		Error, percent
	Experimental	Theoretical		Experimental	Theoretical	
First	43.3	46.4	7.16	52.2	56.70	8.43
Second	88.8	105.3	18.58	91.7	103.4	12.77
Third	122.8	150.0	22.15	131.1	166.6	27.08
Fourth	164.2	202.0	23.02	169.2	216.5	27.95

TABLE VII.- THE ψ COEFFICIENTS FOR SYMMETRIC AND ANTISYMMETRIC MODES

Station, n	First symmetric mode			First antisymmetric mode		
	$\psi_{0,n}$	$\psi_{1,n}$	$\psi_{2,n}$	$\psi_{0,n}$	$\psi_{1,n}$	$\psi_{2,n}$
0	-1.4862	0.024457	-0.00005546	0	0	0
1	-1.3789	.023320	-.00005404	-.0312	.005752	.00000017
2	-1.0651	.020134	-.00005258	-.1154	.013131	-.00001392
3	-.5229	.014939	-.00005700	-.2687	.021039	-.00002562
4	.2582	.007699	-.00007280	-.5137	.028935	-.00002058
5	1.2596	-.001205	-.00010434	-.8625	.036493	.00001118
6	2.4220	-.011701	-.00009519	-1.2995	.043408	.00006029
7	3.6672	-.014848	-.00069212	-1.7963	.045575	.00050698

Station, n	Second symmetric mode			Second antisymmetric mode		
	$\psi_{0,n}$	$\psi_{1,n}$	$\psi_{2,n}$	$\psi_{0,n}$	$\psi_{1,n}$	$\psi_{2,n}$
0	0.2255	-0.009340	0.00012448	0	0	0
1	.2154	-.010401	.00013217	.3181	-.006477	-.00000030
2	.1974	-.013968	.00015982	.6018	-.013888	.00001913
3	.1804	-.019120	.00019049	.7396	-.019110	.00004005
4	.1983	-.025141	.00020134	.6272	-.019885	.00005835
5	.2954	-.031593	.00016630	.1908	-.014828	.00008543
6	.4930	-.037493	.00003626	-.5527	-.004515	.00014013
7	.7923	-.041011	-.00052598	-1.5264	.003366	.00100000

Station, n	Third symmetric mode			Third antisymmetric mode		
	$\psi_{0,n}$	$\psi_{1,n}$	$\psi_{2,n}$	$\psi_{0,n}$	$\psi_{1,n}$	$\psi_{2,n}$
0	-0.0682	-0.005360	0.00009133	0	0	0
1	.0204	-.006366	.00009484	-.0643	-.001502	.00000042
2	.1029	-.008858	.00010193	-.1578	.002960	-.00006281
3	.2486	-.011115	.00009855	-.2096	.012590	-.00018514
4	.3240	-.011129	.00007847	-.2107	.026305	-.00033897
5	.2105	-.006905	.00005602	-.2266	.041626	-.00043593
6	-.1625	.001761	.00009912	-.3680	.053467	-.00021608
7	-.8011	.010870	.00093706	-.7626	.062547	.00100000

Station, n	Fourth symmetric mode			Fourth antisymmetric mode		
	$\psi_{0,n}$	$\psi_{1,n}$	$\psi_{2,n}$	$\psi_{0,n}$	$\psi_{1,n}$	$\psi_{2,n}$
0	0.4506	-0.025574	0.00025835	0	0	0
1	.3874	-.023308	.00023509	-.0964	.002070	-.00000012
2	.1998	-.014407	.00015347	-.1062	.000798	.00002517
3	-.0619	.000218	.00000601	-.0097	-.003736	.00006835
4	-.2976	.018320	-.00018550	.1522	-.009523	.00010543
5	-.3649	.033068	-.00033811	.2373	-.011913	.00010629
6	-.1756	.035897	-.00028145	.0574	-.005948	.00009922
7	.2303	.029159	-.00035149	-.5128	.007359	.00096160

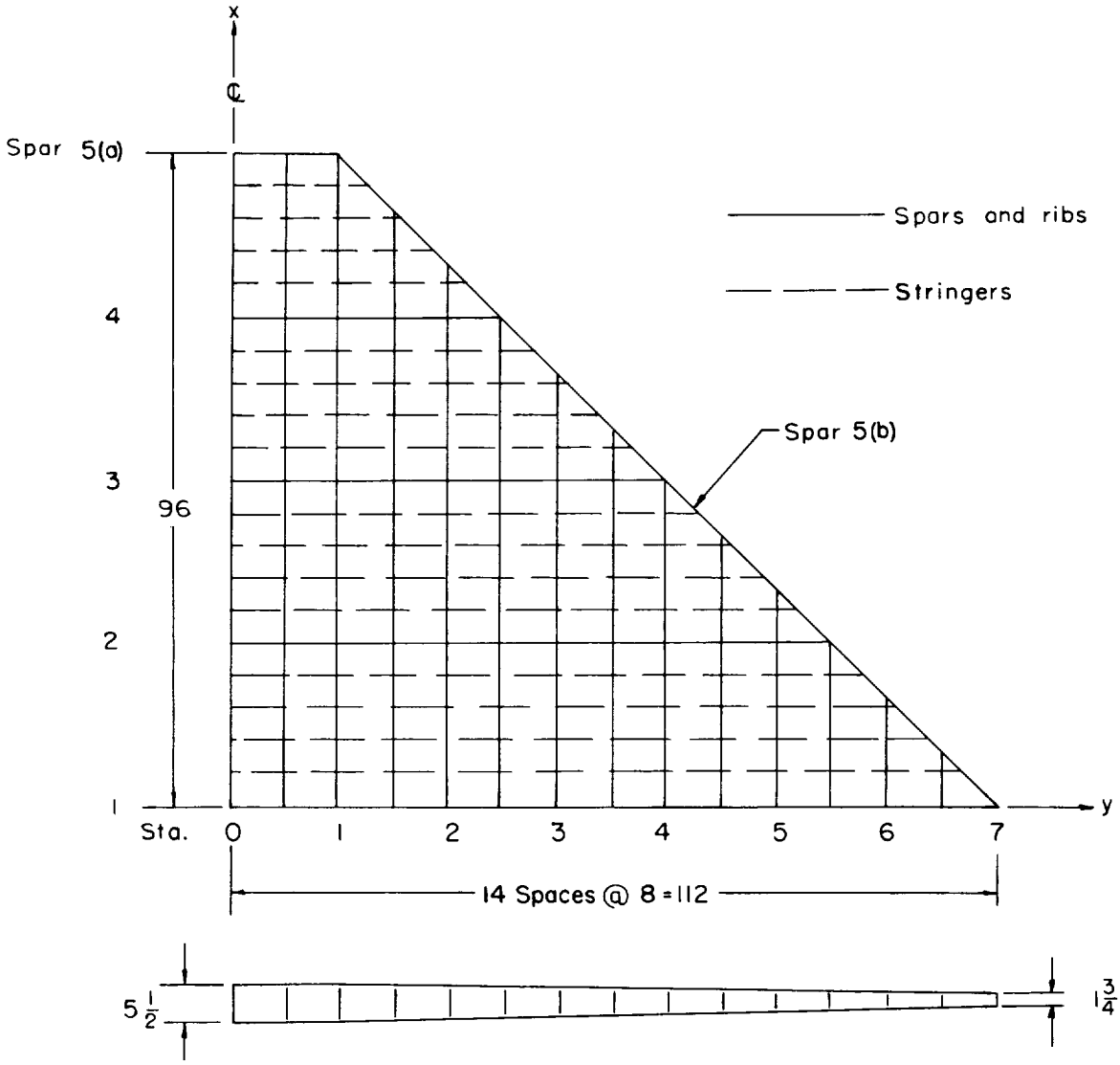

Figure 1.- Diagram of wing specimen showing construction, stations used in the analysis, and coordinate system.

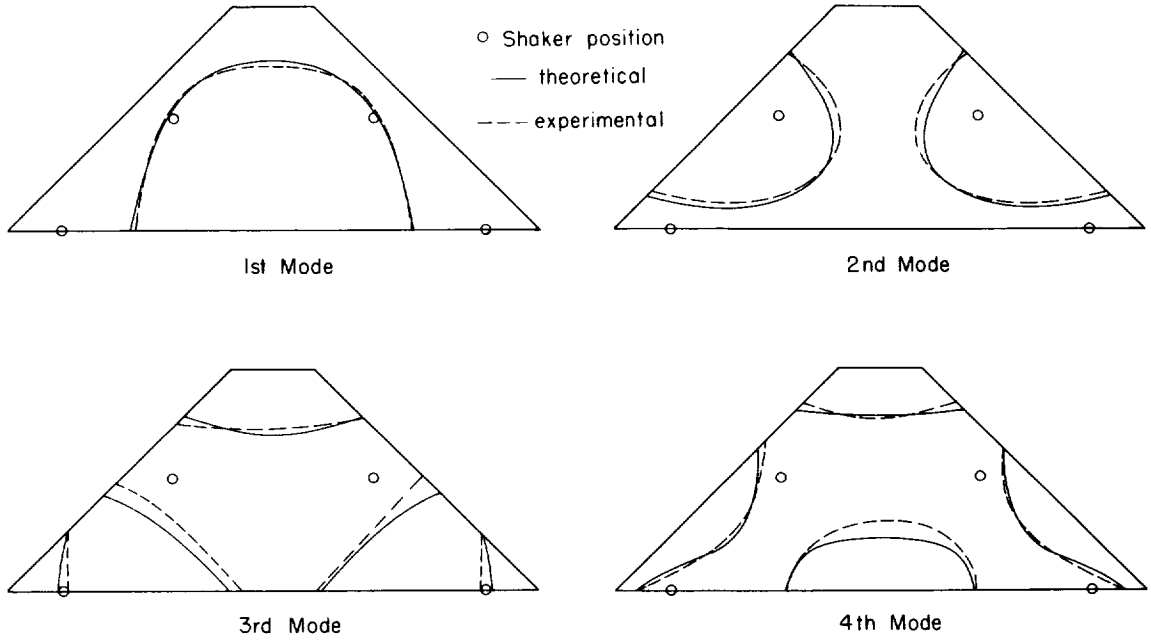

(a) Symmetric modes.

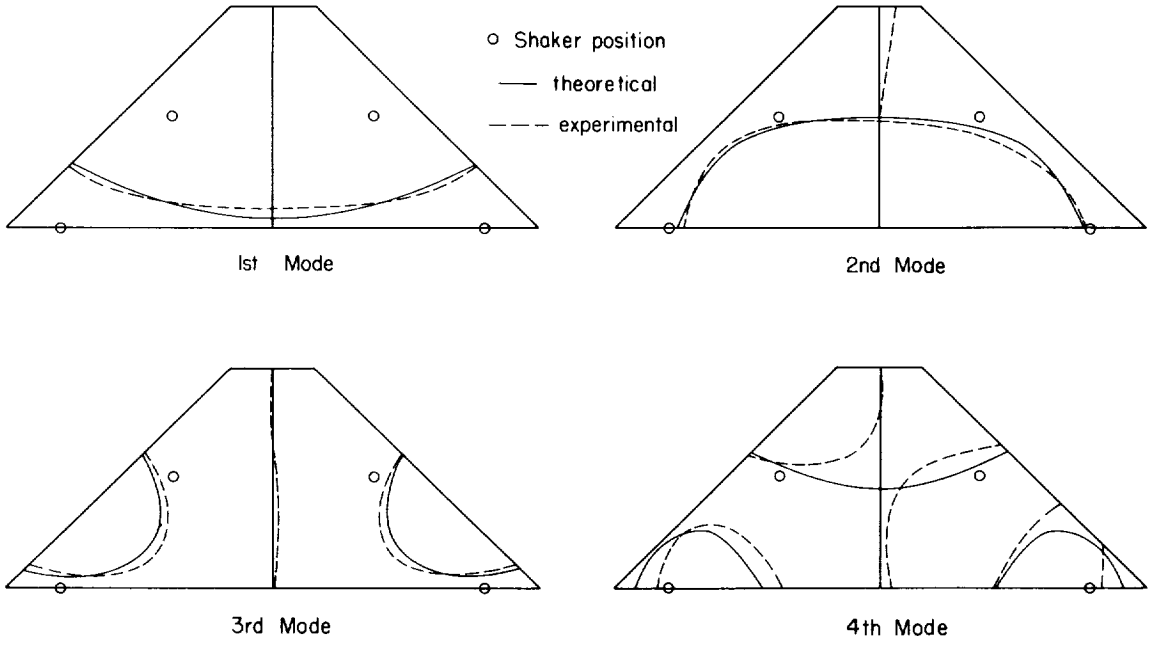

(b) Antisymmetric modes.

Figure 2.- Node-line patterns for free-free natural modes.

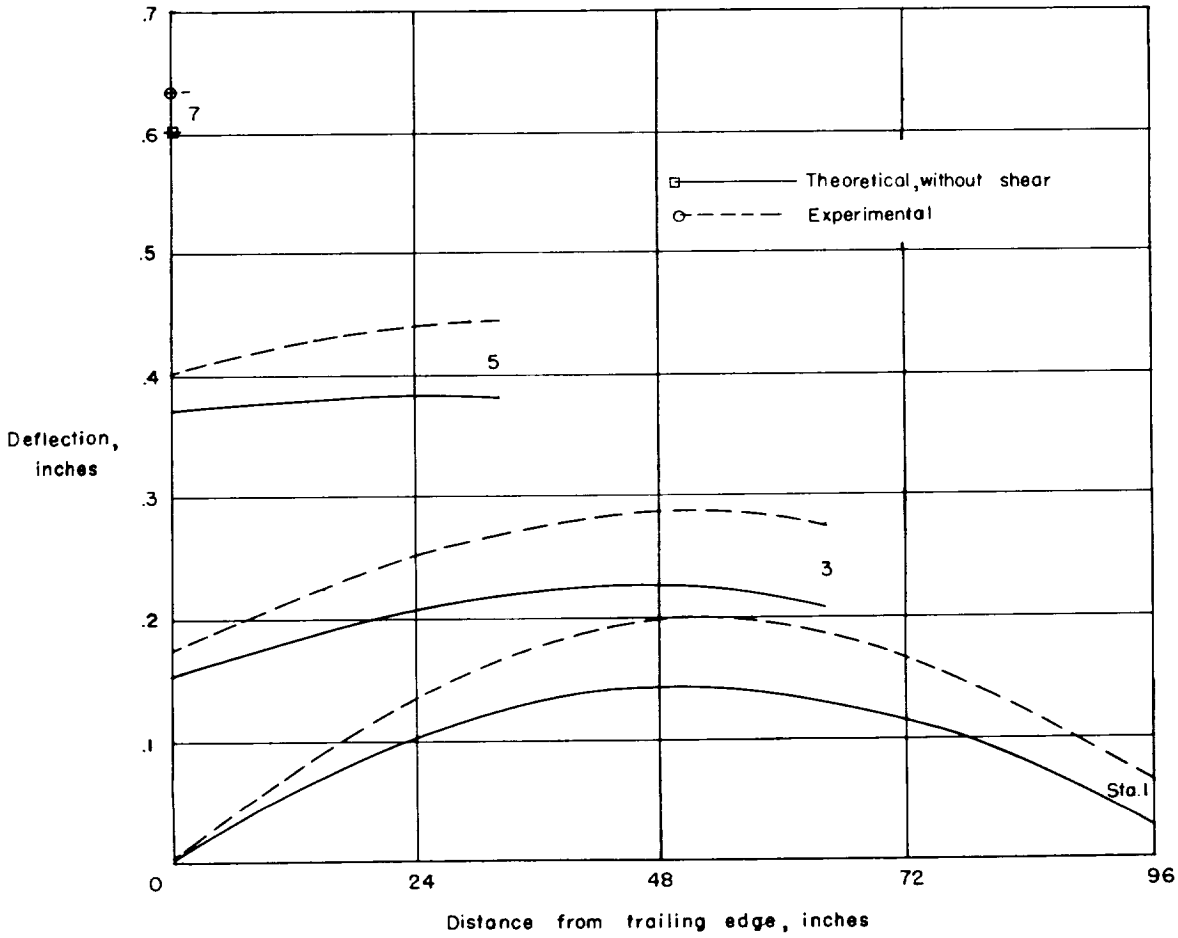

(a) Three-point support.

Figure 3.- Deflection of delta-wing specimen under uniform load of 1 psi.

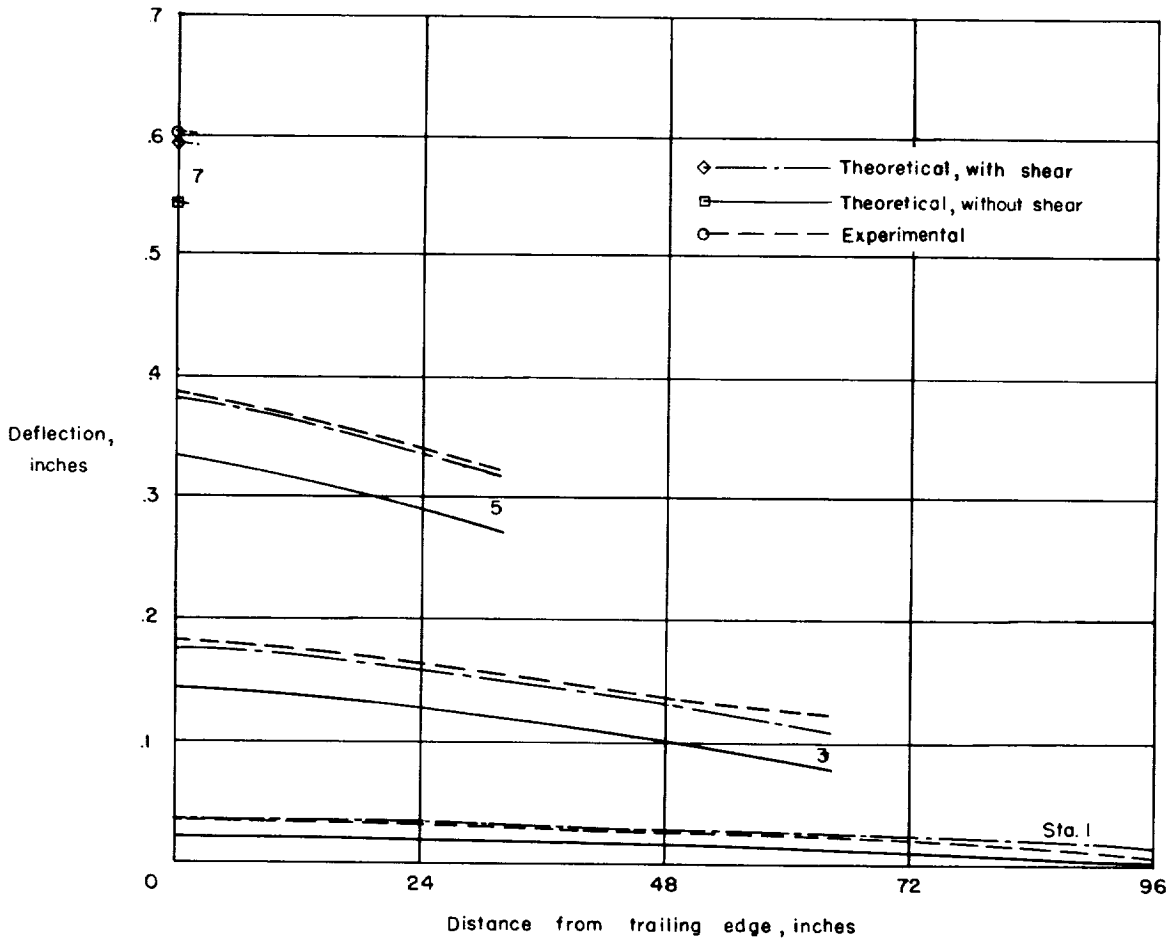

(b) Cantilever support.

Figure 3.- Concluded.

NASA MEMO 2-1-59L
National Aeronautics and Space Administration.
APPLICATION OF THE METHOD OF STEIN AND SANDERS TO THE CALCULATION OF VIBRATION CHARACTERISTICS OF A 45° DELTA-WING SPECIMEN. John M. Hedgepeth and Paul G. Waner, Jr. February 1959. 26p. diagrs., tabs.
(NASA MEMORANDUM 2-1-59L)

Generalized influence coefficients are calculated by the method of NACA TN 3640 for a large-scale, built-up, 45° delta-wing specimen. These are used together with appropriate generalized masses to obtain the natural modes and frequencies in symmetric and antisymmetric free-free vibration. The resulting frequencies are compared with those obtained experimentally and are found to be consistently high. Possible sources of the disparities are discussed.

Copies obtainable from NASA, Washington

1. Vibration and Flutter - Wings and Ailerons (4.2.1)
2. Loads and Stresses, Structural (4.3.7)

I. Hedgepeth, John Mills
II. Waner, Paul G., Jr.
III. NASA MEMO 2-1-59L

NASA

NASA MEMO 2-1-59L
National Aeronautics and Space Administration.
APPLICATION OF THE METHOD OF STEIN AND SANDERS TO THE CALCULATION OF VIBRATION CHARACTERISTICS OF A 45° DELTA-WING SPECIMEN. John M. Hedgepeth and Paul G. Waner, Jr. February 1959. 26p. diagrs., tabs.
(NASA MEMORANDUM 2-1-59L)

Generalized influence coefficients are calculated by the method of NACA TN 3640 for a large-scale, built-up, 45° delta-wing specimen. These are used together with appropriate generalized masses to obtain the natural modes and frequencies in symmetric and antisymmetric free-free vibration. The resulting frequencies are compared with those obtained experimentally and are found to be consistently high. Possible sources of the disparities are discussed.

Copies obtainable from NASA, Washington

1. Vibration and Flutter - Wings and Ailerons (4.2.1)
2. Loads and Stresses, Structural (4.3.7)

I. Hedgepeth, John Mills
II. Waner, Paul G., Jr.
III. NASA MEMO 2-1-59L

NASA

NASA MEMO 2-1-59L
National Aeronautics and Space Administration.
APPLICATION OF THE METHOD OF STEIN AND SANDERS TO THE CALCULATION OF VIBRATION CHARACTERISTICS OF A 45° DELTA-WING SPECIMEN. John M. Hedgepeth and Paul G. Waner, Jr. February 1959. 26p. diagrs., tabs.
(NASA MEMORANDUM 2-1-59L)

Generalized influence coefficients are calculated by the method of NACA TN 3640 for a large-scale, built-up, 45° delta-wing specimen. These are used together with appropriate generalized masses to obtain the natural modes and frequencies in symmetric and antisymmetric free-free vibration. The resulting frequencies are compared with those obtained experimentally and are found to be consistently high. Possible sources of the disparities are discussed.

Copies obtainable from NASA, Washington

1. Vibration and Flutter - Wings and Ailerons (4.2.1)
2. Loads and Stresses, Structural (4.3.7)

I. Hedgepeth, John Mills
II. Waner, Paul G., Jr.
III. NASA MEMO 2-1-59L

NASA

NASA MEMO 2-1-59L
National Aeronautics and Space Administration.
APPLICATION OF THE METHOD OF STEIN AND SANDERS TO THE CALCULATION OF VIBRATION CHARACTERISTICS OF A 45° DELTA-WING SPECIMEN. John M. Hedgepeth and Paul G. Waner, Jr. February 1959. 26p. diagrs., tabs.
(NASA MEMORANDUM 2-1-59L)

Generalized influence coefficients are calculated by the method of NACA TN 3640 for a large-scale, built-up, 45° delta-wing specimen. These are used together with appropriate generalized masses to obtain the natural modes and frequencies in symmetric and antisymmetric free-free vibration. The resulting frequencies are compared with those obtained experimentally and are found to be consistently high. Possible sources of the disparities are discussed.

Copies obtainable from NASA, Washington

1. Vibration and Flutter - Wings and Ailerons (4.2.1)
2. Loads and Stresses, Structural (4.3.7)

I. Hedgepeth, John Mills
II. Waner, Paul G., Jr.
III. NASA MEMO 2-1-59L

NASA